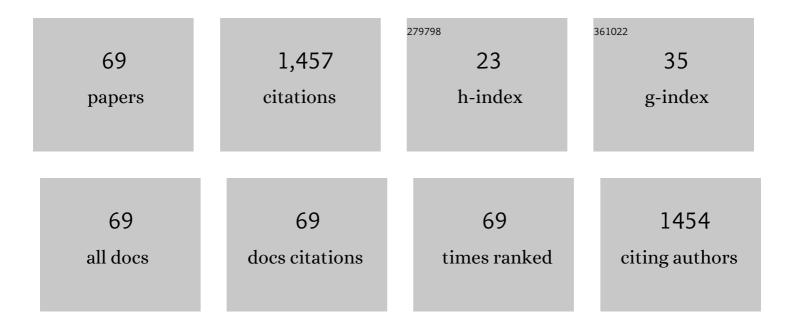


List of Publications by Year in descending order

Source: https://exaly.com/author-pdf/4177777/publications.pdf Version: 2024-02-01



ΒΛΝΙΙΛ

#	Article	IF	CITATIONS
1	Subnanometer Bimetallic Platinum–Zinc Clusters in Zeolites for Propane Dehydrogenation. Angewandte Chemie - International Edition, 2020, 59, 19450-19459.	13.8	221
2	What Makes Hydroxamate a Promising Anchoring Group in Dye-Sensitized Solar Cells? Insights from Theoretical Investigation. Journal of Physical Chemistry Letters, 2014, 5, 3992-3999.	4.6	61
3	Synthesis of MoSe ₂ /CoSe ₂ Nanosheets for NIRâ€Enhanced Chemodynamic Therapy via Synergistic Inâ€Situ H ₂ O ₂ Production and Activation. Advanced Functional Materials, 2021, 31, 2008420.	14.9	59
4	NIR-Driven Intracellular Photocatalytic O ₂ Evolution on Z-Scheme Ni ₃ S ₂ /Cu _{1.8} S@HA for Hypoxic Tumor Therapy. ACS Applied Materials & Interfaces, 2021, 13, 9604-9619.	8.0	50
5	Fine-tuning Ï€-spacer for high efficiency performance DSSC: A theoretical exploration with <mml:math altimg="si1.gif" overflow="scroll" xmlns:mml="http://www.w3.org/1998/Math/MathML"><mml:mi><mml:mi>D</mml:mi><mml:mo>â² </mml:mo><mml:mi>Ï€</mml:mi>iml:mo>â² <mml:mi>iml:mo>â² <mml:mi>iml:mo>â² <mml:mi>iml:mo>â² <mml:mi>iml:mo>â² <mml:mi>iml:mo>â² </mml:mi></mml:mi></mml:mi></mml:mi></mml:mi></mml:mi></mml:math>	~ 3.7 mml:m	10 ⁴⁹ mml:mi
6	Subnanometer Bimetallic Platinum–Zinc Clusters in Zeolites for Propane Dehydrogenation. Angewandte Chemie, 2020, 132, 19618-19627.	2.0	47
7	Comparative Ab Initio Calculations of ReO3, SrZrO3, BaZrO3, PbZrO3 and CaZrO3 (001) Surfaces. Crystals, 2020, 10, 745.	2.2	46
8	Novel N–Br Bond-Containing <i>N</i> -Halamine Nanofibers with Antibacterial Activities. ACS Biomaterials Science and Engineering, 2018, 4, 2193-2202.	5.2	44
9	Comparative Hybrid Hartree-Fock-DFT Calculations of WO2-Terminated Cubic WO3 as Well as SrTiO3, BaTiO3, PbTiO3 and CaTiO3 (001) Surfaces. Crystals, 2021, 11, 455.	2.2	44
10	Investigation of Properties of Mg _{<i>n</i>} Clusters and Their Hydrogen Storage Mechanism: A Study Based on DFT and a Global Minimum Optimization Method. Journal of Physical Chemistry A, 2015, 119, 3636-3643.	2.5	40
11	Comprehensive Investigation into Luminescent Properties of Ir(III) Complexes: An Integrated Computational Study of Radiative and Nonradiative Decay Processes. Inorganic Chemistry, 2018, 57, 6561-6570.	4.0	40
12	Anionic ancillary ligands in cyclometalated Ru(<scp>ii</scp>) complex sensitizers improve photovoltaic efficiency of dye-sensitized solar cells: insights from theoretical investigations. Journal of Materials Chemistry A, 2017, 5, 15567-15577.	10.3	33
13	Theoretical study on hydrogen storage capacity of expanded h-BN systems. Computational Materials Science, 2017, 139, 335-340.	3.0	32
14	Theoretical studies on the spectroscopic properties of porphyrin derivatives for dye-sensitized solar cell application. RSC Advances, 2015, 5, 33653-33665.	3.6	30
15	Tendencies in ABO3 Perovskite and SrF2, BaF2 and CaF2 Bulk and Surface F-Center Ab Initio Computations at High Symmetry Cubic Structure. Symmetry, 2021, 13, 1920.	2.2	30
16	The influence of a dye–TiO ₂ interface on DSSC performance: a theoretical exploration with a ruthenium dye. RSC Advances, 2016, 6, 81976-81982.	3.6	28
17	Novel Carbon Nanotubes Rolled from 6,6,12-Graphyne: Double Dirac Points in 1D Material. Journal of Physical Chemistry C, 2017, 121, 14835-14844.	3.1	28
18	The effect of relative position of the π -spacer center between donor and acceptor on the overall performance of D- π -A dye: a theoretical study with organic dye. Electrochimica Acta, 2017, 241, 440-448.	5.2	27

Ran Jia

#	Article	IF	CITATIONS
19	How does graphene enhance the photoelectric conversion efficiency of dye sensitized solar cells? An insight from a theoretical perspective. Journal of Materials Chemistry A, 2019, 7, 2730-2740.	10.3	26
20	A novel T-C ₃ N and seawater desalination. Nanoscale, 2020, 12, 5055-5066.	5.6	26
21	Online Wear Particle Detection Sensors for Wear Monitoring of Mechanical Equipment—A Review. IEEE Sensors Journal, 2022, 22, 2930-2947.	4.7	26
22	Certain doping concentrations caused half-metallic graphene. Journal of Saudi Chemical Society, 2017, 21, 111-117.	5.2	24
23	DFT/TD-DFT calculations on the sensing mechanism of a dual response near-infrared fluorescent chemosensor for superoxide anion and hydrogen polysulfides: photoinduced electron transfer. RSC Advances, 2016, 6, 104735-104741.	3.6	23
24	Ab initio calculations of CaZrO3 (011) surfaces: systematic trends in polar (011) surface calculations of ABO3 perovskites. Journal of Materials Science, 2020, 55, 203-217.	3.7	23
25	Ab Initio Computations of O and AO as well as ReO2, WO2 and BO2-Terminated ReO3, WO3, BaTiO3, SrTiO3 and BaZrO3 (001) Surfaces. Symmetry, 2022, 14, 1050.	2.2	23
26	The effect of D–[D _e –π–A] _n (n = 1, 2, 3) type dyes on the overall performance of DSSCs: a theoretical investigation. Journal of Materials Chemistry C, 2017, 5, 7510-7520.	5.5	22
27	Pathway of in situ polymerization of 1,3-dioxolane in LiPF6 electrolyte on Li metal anode. Materials Today Energy, 2021, 21, 100730.	4.7	22
28	Metal doped fullerene complexes as promising drug delivery materials against COVID-19. Chemical Papers, 2021, 75, 6487-6497.	2.2	19
29	Novel 2D boron nitride with optimal direct band gap: A theoretical prediction. Applied Surface Science, 2022, 578, 151929.	6.1	19
30	Giant piezoelectricity in B/N doped 4,12,2-graphyne. Applied Surface Science, 2020, 499, 143800.	6.1	18
31	B N counterpart of biphenylene network: A theoretical investigation. Applied Surface Science, 2022, 598, 153674.	6.1	18
32	Arranging strategies for A-site cations: impact on the stability and carrier migration of hybrid perovskite materials. Inorganic Chemistry Frontiers, 2020, 7, 1741-1749.	6.0	17
33	Origin of the deep band-gap state in <mml:math xmlns:mml="http://www.w3.org/1998/Math/MathML"><mml:msub><mml:mi>TiO</mml:mi><mml:mn>2(110): <mml:math xmlns:mml="http://www.w3.org/1998/Math/MathML"><mml:mrow><mml:mi>d</mml:mi>dd</mml:mrow></mml:math </mml:mn></mml:msub></mml:math 	3.2	14
34	bonds between Ti-Ti pairs. Physical Review B, 2010, 98, . Computational and biological investigation of the soybean lecithin–gallic acid complex for ameliorating alcoholic liver disease in mice with iron overload. Food and Function, 2019, 10, 5203-5214.	4.6	14
35	Metallic subnanometer porous silicon: A theoretical prediction. Physical Review B, 2021, 103, .	3.2	13
36	Overall direct photocatalytic water-splitting on <i>C</i> 2 <i>mm</i> -graphyne: a novel two-dimensional carbon allotrone, Journal of Materials Chemistry C, 2022, 10, 10843-10852	5.5	13

Ran Jia

#	Article	IF	CITATIONS
37	Iron oxides with a reverse spinel structure: impact of active sites on molecule adsorption. Inorganic Chemistry Frontiers, 2019, 6, 2810-2816.	6.0	12
38	Dipoles in 4,12,4-graphyne. Applied Surface Science, 2021, 545, 148991.	6.1	12
39	The correlations among the fragility of supercooled liquids, the fragility of superheated melts, and the glass-forming ability for marginal metallic glasses. Journal of Applied Physics, 2009, 105, 024304.	2.5	11
40	From determination of the fugacity coefficients to estimation of hydrogen storage capacity: A convenient theoretical method. International Journal of Hydrogen Energy, 2015, 40, 10908-10917.	7.1	11
41	Assembly of polysubstituted chiral cyclopropylamines <i>via</i> highly enantioselective Cu-catalyzed three-component cyclopropene alkenylamination. Chemical Communications, 2020, 56, 12250-12253.	4.1	11
42	Designation and Match of Nonâ€Fullerene Acceptors with Xâ€Shaped Donors toward Organic Solar Cells. ChemistrySelect, 2019, 4, 3654-3664.	1.5	10
43	Regulating vibrational modes to improve quantum efficiency: insights from theoretical calculations on iridium(<scp>iii</scp>) complexes bearing tridentate NCN and NNC chelates. Dalton Transactions, 2019, 48, 5064-5071.	3.3	9
44	The molecular mechanism behind protein kinase B natural mutant E17K affecting the allosteric inhibitor sensitivity: a molecular dynamics simulation study. Journal of Biomolecular Structure and Dynamics, 2021, 39, 1-14.	3.5	9
45	Exploring the sensitization properties of thienyl-functionalized tripyrrole Ru(II) complexes on TiO2 (101) surface: a theoretical study. Theoretical Chemistry Accounts, 2015, 134, 1.	1.4	7
46	3D-Graphene/Boron Nitride-stacking Material: a Fundamental van der Waals Heterostructure. Chemical Research in Chinese Universities, 2018, 34, 434-439.	2.6	7
47	Theoretical study on the influence of electric field direction on the photovoltaic performance of aryl amine organic dyes for dye-sensitized solar cells. New Journal of Chemistry, 2019, 43, 651-661.	2.8	7
48	How does fluoride enhance hydroxyapatite? A theoretical understanding. Applied Surface Science, 2022, 586, 152753.	6.1	7
49	Molecular Dynamics Simulation Investigation of the Binding and Interaction of the EphA6–Odin Protein Complex. Journal of Physical Chemistry B, 2022, 126, 4914-4924.	2.6	7
50	Theoretical studies on the absorption spectra and intramolecular charge transfer of push-pull zinc porphyrin dyes for dye-sensitized solar cells. Chemical Research in Chinese Universities, 2015, 31, 276-280.	2.6	6
51	DFT and TDDFT Studies of Non-Fullerene Organometallic Based Acceptors for Organic Photovoltaics. Journal of Inorganic and Organometallic Polymers and Materials, 2021, 31, 1676-1687.	3.7	6
52	Edge modified phosphorene nanoribbon heterojunctions: promising metal-free photocatalysts for direct overall water splitting. Journal of Materials Science, 2022, 57, 5482-5496.	3.7	6
53	Frontispiece: Subnanometer Bimetallic Platinum–Zinc Clusters in Zeolites for Propane Dehydrogenation. Angewandte Chemie - International Edition, 2020, 59, .	13.8	5
54	Co-doping with boron and nitrogen impurities in T-carbon. Journal of Saudi Chemical Society, 2020, 24, 857-864.	5.2	5

Ran Jia

#	Article	IF	CITATIONS
55	Studies on covalent functionalization of single layer black phosphorus from GW calculations based on the many body perturbation theory. Electronic Structure, 2020, 2, 025005.	2.8	5
56	Fabrication of three-component hydrogen-bonded covalent-organic polymers for ciprofloxacin decontamination from water: adsorption mechanism and modeling. Materials Today Chemistry, 2021, 20, 100463.	3.5	5
57	How does the porphyrin-like vacancy affect the spectral properties of graphene quantum dots? A theoretical study. Journal of Physics Condensed Matter, 2020, 32, 155902.	1.8	4
58	Comparative <i>ab initio</i> calculations of SrTiO3, BaTiO3, PbTiO3, and SrZrO3 (001) and (111) surfaces as well as oxygen vacancies. Low Temperature Physics, 2022, 48, 80-88.	0.6	4
59	Carbon ene-yne working in oxygenator: A theoretical study. Diamond and Related Materials, 2022, 125, 108991.	3.9	4
60	Nickel-catalyzed carboxylation of aryl zinc reagent with CO2: A theoretical and experimental study. Journal of CO2 Utilization, 2019, 29, 262-270.	6.8	3
61	Configuration effect in polyoxometalate-based dyes on the performance of DSSCs: an insight from a theoretical perspective. Physical Chemistry Chemical Physics, 2020, 22, 16032-16039.	2.8	3
62	Comparative Hybrid Hartree-Fock-DFT Calculations of ReO ₃ , SrTiO ₃ , BaTiO ₃ , PbTiO ₃ and CaTiO ₃ (001) Surfaces. Integrated Ferroelectrics, 2021, 220, 9-17.	0.7	3
63	Study on the Sensitivity of Detachable Wear Particle Sensor Based on Iron-Based Amorphous Soft Magnetic Rings. IEEE Sensors Journal, 2022, 22, 12708-12718.	4.7	3
64	Why HSâ^' and CNâ^' can be detected by different chemosensors with similar structures: a quantum mechanics and molecular dynamics study. RSC Advances, 2016, 6, 63548-63558.	3.6	2
65	Theoretical investigation of the influence of different electric field directions and strengths on a POM-based dye for dye-sensitized solar cells. Materials Chemistry Frontiers, 2021, 5, 929-936.	5.9	2
66	Penta-silicon carbide: A theoretical investigation. Materials Science and Engineering B: Solid-State Materials for Advanced Technology, 2022, 281, 115740.	3.5	1
67	Theoretical investigations of the heavily boron doped pentadiamond. Diamond and Related Materials, 2022, 126, 109127.	3.9	1
68	Investigating detailed mechanism of hydrogen molecules adsorbing on singleâ€wall carbon nanotubes using fitted force field parameters containing carbon–carbon interactions. Journal of Computational Chemistry, 2019, 40, 1073-1083.	3.3	0
69	Frontispiz: Subnanometer Bimetallic Platinum–Zinc Clusters in Zeolites for Propane Dehydrogenation. Angewandte Chemie, 2020, 132, .	2.0	0